

IDENTIFICATION OF STIFFNESS AND DAMPING COEFFICIENTS OF AEROSTATIC JOURNAL BEARING

Jan Kozánek*, Jiří Šimek**, Pavel Steinbauer, Aleš Bílkovský***

Paper deals with subject of identification of aerostatic journal bearings dynamic properties with use of Rotor Kit Bently Nevada superstructure. Different bearing types were experimentally investigated and their static and dynamic characteristics were identified. Various methods of identification were used and spectral and modal properties of the system were calculated. Computer program was revised on the basis of experimental data. The influence of non-diagonal stiffness and damping elements was investigated by numeric simulation.

Keywords: aerostatic journal bearings, stiffness and damping, Rotor Kit Bently Nevada, experimental stand, mathematical model, spectral and modal properties

1. Introduction

Project of identification of aerostatic journal bearing dynamic properties was started in 2006. Super-structure of Rotor Kit Bently Nevada (RK) was designed and manufactured [1,2] and after some modifications [3] successfully used for identification of stiffness and damping coefficients. Methods of identification were developed to enable identification even in cases of not quite ideal harmonic signals. Comparison of measured and calculated data enabled to revise computer program and to achieve much better agreement between theory and experiment. The influence of non-diagonal elements of stiffness and damping matrices on spectral properties was investigated, too.

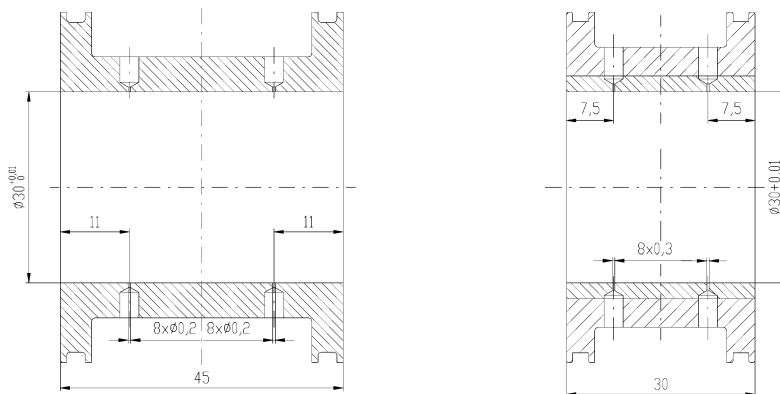


Fig.1: Test aerostatic journal bearings – variant 1 (left) and 2 (right)

* Ing. J. Kozánek, CSc., Institute of Thermomechanics AS CR, v.v.i., Dolejškova 5, 182 00 Praha 8

** Ing. J. Šimek, CSc., Techlab s.r.o., Sokolovská 207, 190 00 Praha 9

*** Ing. P. Steinbauer, Ph.D., Ing. A. Bílkovský, CTU in Prague, FME, Technická 4, 160 00 Praha 6

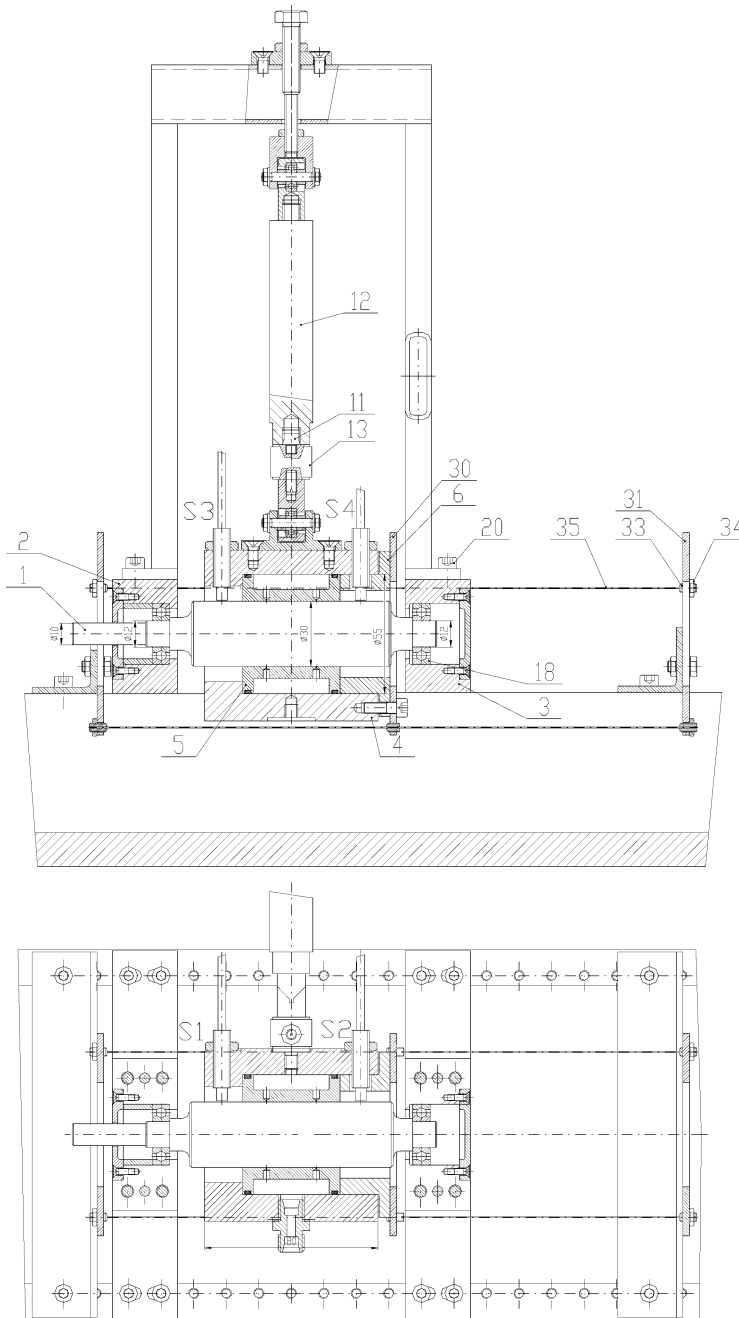


Fig.2: Superstructure of Rotor Kit equipped with vertically (up) and horizontally (down) oriented piezoactuators for excitation of test bearing

2. Test stand and test bearings

Two test bearings were used, both with two feeding planes (two rows of feeding orifices – see Fig.1), because bearing with one feeding plane in the middle is more sensitive to parasitic forces.

Both bearings had 8 orifices symmetrically distributed around periphery: bearing 1 with l/D ratio of 1.5 and radial clearance of 0.04 mm had orifices 0.2 mm in diameter, bearing 2 with l/D ratio of 1.0 and radial clearance of 0.025 mm was equipped with orifices 0.3 mm in diameter. When identifying bearing characteristics, the journal can move within about 50% of radial clearance, so that some space for harmonic excitation is left. One can imagine extremely high demands on accuracy of adjusting the bearing position during tests with piezoactuator static offset. Several structural modifications had to be built and tested to attain required translational motion of the test head.

Cross section of test stand is shown in Fig.2. Rigid shaft 1 is supported in two precise ball bearings 18 with the casings 2, 3 fastened to RK frame. Aerostatic test bearing 5,

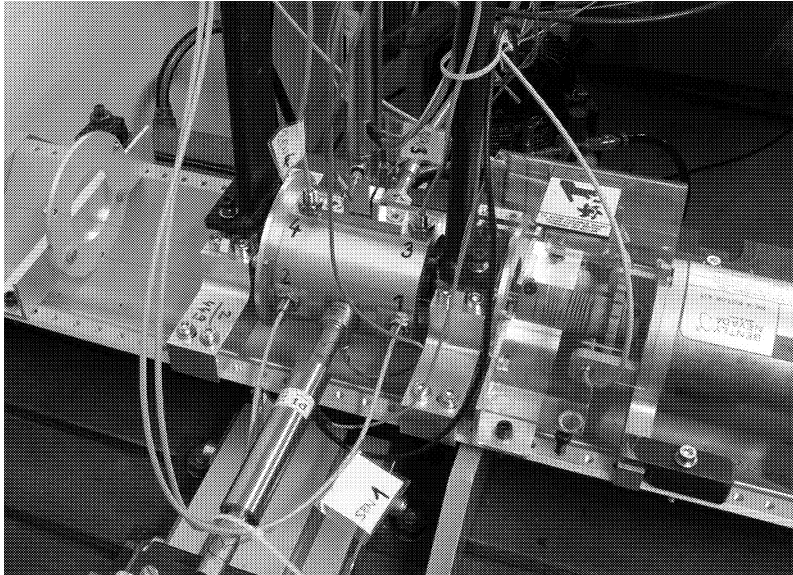


Fig.3: Detail of Rotor Kit superstructure



Fig.4: Instrumentation for experiment control and data acquisition

enclosed in test head 4 located between supporting bearings, can be excited by vertically and horizontally oriented piezoactuators 12. Exciting forces are transferred to test bearing via load cells 13, thus enabling to measure instant values of dynamic force. Test bearing response is observed by two pairs of relative sensors S1, S2 and S3, S4. Parallelism of test bearing motion relative to shaft surface is secured by suspension, consisting of three thin strings 35 anchored at test head disk 30 and two disks 31 fastened to the RK frame. Proper alignment of the test head with the shaft is achieved by means of threaded pins 33 and nuts 34. Detail of the test stand is presented in Fig. 3, instrumentation necessary for experiment control and data recording is shown in Fig. 4.

3. Method of dynamic characteristics identification

Coefficients of stiffness and damping matrices were identified from dynamic model shown in Fig. 5, which was in more detail presented e.g. at [2], frequency of rotation $\omega = 2\pi n/60$ and n signifies rpm.

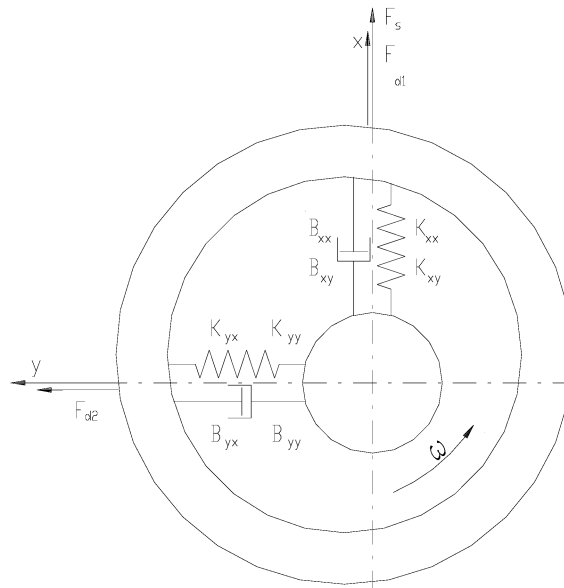


Fig.5: Simplified dynamic model of the test stand

The real part of the time-response $\tilde{\mathbf{q}}(t) = [x(t) \ y(t)]^T$ of the test bearing relative to the shaft on the complex harmonic excitation force with the frequency $\Omega = 2\pi f$, $f > 0$

$$\mathbf{f}(t) = \begin{bmatrix} f_x(t) \\ f_y(t) \end{bmatrix} = \begin{bmatrix} f_x \\ f_y \end{bmatrix} e^{i\Omega t} = \mathbf{f} e^{i\Omega t}, \quad \mathbf{f} \in R^2, \quad i = \sqrt{-1}, \quad \Omega > 0 \quad (1)$$

was evaluated from measured discretized signal in the first step as the simple linear (in real parameters $\mathbf{q}_0, \mathbf{q}_S, \mathbf{q}_C \in R^2$) and non-linear (related to Ω) least squares regression problems

$$\tilde{\mathbf{q}}(t) = \mathbf{q}_0 + \mathbf{q}_S \sin(\Omega t) + \mathbf{q}_C \cos(\Omega t) \quad (2)$$

and transformed into ‘complex amplitude form’

$$\mathbf{q}(t) = \mathbf{q} e^{i\Omega t}, \quad \mathbf{q} = \mathbf{q}_C - i\mathbf{q}_S \in C^2 \quad (3)$$

corresponding to the complex excitation force (1). The equation of motion in harmonic regime and in amplitude form is

$$\mathbf{K}\mathbf{q} + i\Omega\mathbf{B}\mathbf{q} - \Omega^2\mathbf{M}\mathbf{q} = \mathbf{f}, \quad (4)$$

where real matrices \mathbf{K} , \mathbf{B} , $\mathbf{M} \in R^{2,2}$ are matrices of stiffness, damping and mass. In our case the matrix

$$\mathbf{M} = \begin{bmatrix} M & 0 \\ 0 & M \end{bmatrix},$$

where M is mass of test head with aerostatic bearing, is known. The unknown parameters – elements of matrices

$$\mathbf{K} = \begin{bmatrix} K_{xx} & K_{xy} \\ K_{yx} & K_{yy} \end{bmatrix}, \quad \mathbf{B} = \begin{bmatrix} B_{xx} & B_{xy} \\ B_{yx} & B_{yy} \end{bmatrix},$$

can be identified from the equations (4) for two orthogonal excitation forces \mathbf{f} and for one or more corresponding excitation frequencies Ω using least squares method – see [2].

Higher number of measurements with different excitation frequencies, especially in regions near resonance, should increase robustness of solution. In ideal case it would be also advisable to identify eigenvalues by indirect identification method and to confront these values with eigenvalues corresponding to identified stiffness and damping matrices. It is also possible to determine at first step diagonal elements of stiffness and damping matrices, which are less sensitive to measurement errors, and only in further phase of evaluation to deal with cross coupling terms.

4. Calculated bearing characteristics

Very low frequencies from $f = 0.5$ Hz to $f = 4$ Hz were used to compare ‘quasi-static’ stiffness, defined as a ratio of excitation force amplitude to bearing response amplitude, with calculated values. ‘Quasi-static’ stiffness is practically independent on excitation frequency and for both bearings its measured values are summarized in Table 1.

direction of excitation	stiffness (N.m ⁻¹)			
	bearing 1		bearing 2	
	0.2 MPa	0.4 MPa	0.2 MPa	0.4 MPa
vertical	1.13×10^6	1.54×10^6	1.94×10^6	3.90×10^6
horizontal	—	—	1.00×10^6	3.22×10^6

Tab.1: Measured ‘quasi-static’ stiffness

Difference in stiffness with vertical and horizontal excitation can be explained by varied position of journal in bearing gap. As can be seen from calculated load carrying capacity characteristics in Fig. 6, bearing 1 has practically linear characteristic up to relative eccentricity of about 0.7. On the other hand, characteristic of bearing 2 starts to bend from relative eccentricity of about 0.4. The difference in ‘quasi-static’ values of bearing 2 stiffness can be explained by slightly different value of relative dominant eccentricity in vertical direction. To achieve the same magnitude of eccentricity for both directions of excitation is practically impossible due to above-mentioned small values of bearing gap.

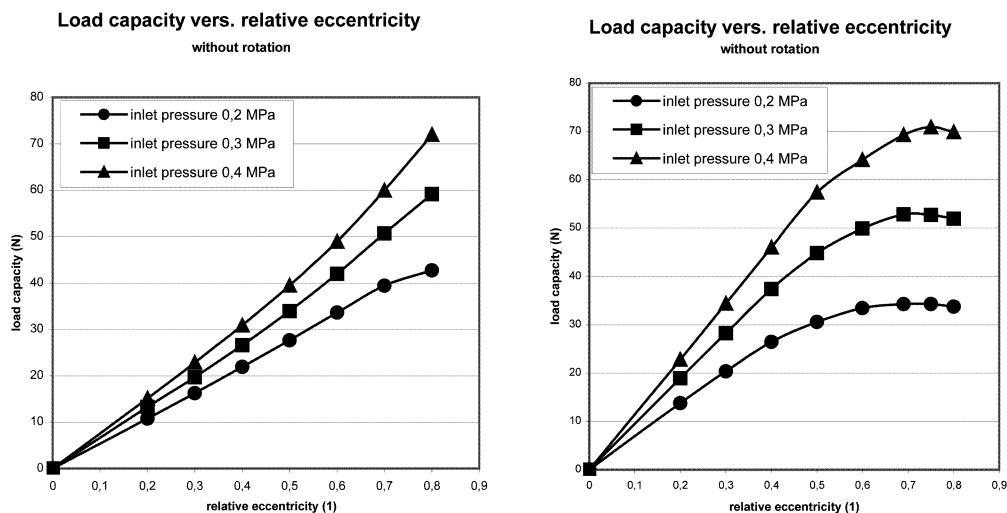


Fig.6: Calculated load capacity of bearing 1 (left) and 2 (right)

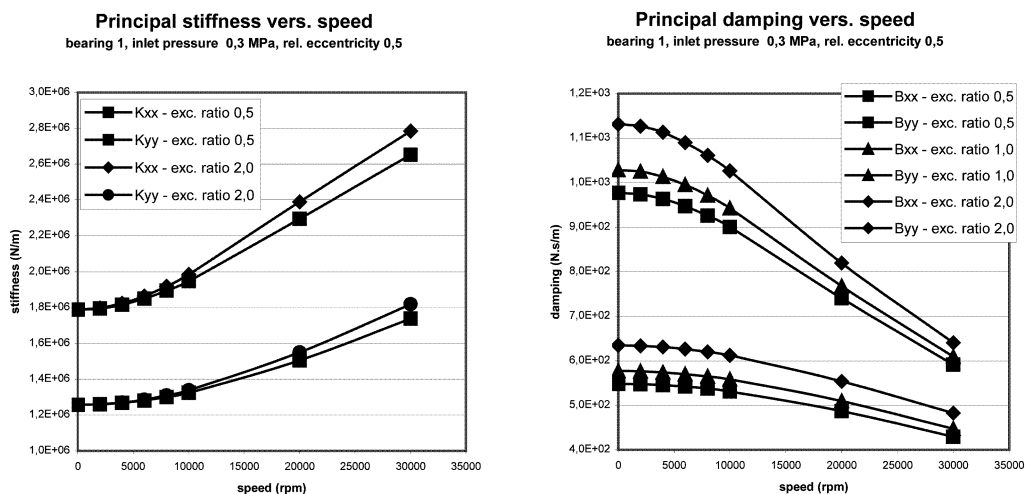


Fig.7: Calculated principal stiffness and damping coefficients of bearing 1

Fig. 7 illustrates influence of speed $n = 60\omega/2\pi$ and excitation ratio $r = \Omega/\omega$ of exciting to rotational frequency for $\omega > 0$ on principal stiffness and damping coefficients. As can be seen, in test regime range (up to $n = 6000$ rpm) the influence of speed is very weak. Stiffness curves for excitation ratio $r = 1.0$ are omitted, because they are very close to those for excitation ratio $r = 2.0$.

5. Some identified stiffness and damping coefficients

Identified stiffness and damping coefficients of test bearing 1 are presented in Table 2 for two values of inlet pressure and relatively broad range of excitation and revolution frequencies. Due to greater bearing width, which made the test more resistant to disturbing phenomena, somewhat better results were obtained with this bearing as compared with bearing 2.

Inlet pressure (MPa)	speed n (rpm)	excitation frequency f (Hz)	ratio r	K_{xx} (N.m ⁻¹)	K_{yy} (N.m ⁻¹)	B_{xx} (N.s.m ⁻¹)	B_{yy} (N.s.m ⁻¹)
0.2	0	5	–	9.52E+05	9.65E+05	525	698
	1000	16.7	1	9.88E+05	9.79E+05	589	465
	2000	66.7	2	9.30E+05	9.79E+05	777	786
	3000	25	0.5	1.00E+06	9.66E+05	457	461
	4000	33.3	0.5	9.84E+05	9.77E+05	401	429
	5000	41.7	0.5	9.51E+05	9.71E+05	500	485
0.4	0	5	–	1.42E+06	1.41E+06	1158	1280
	1000	8.3	0.5	1.43E+06	1.45E+06	1063	556
	2000	16.7	0.5	1.43E+06	1.44E+06	497	471
	3000	25	0.5	1.42E+06	1.42E+06	450	447
	4000	33.3	0.5	1.44E+06	1.45E+06	344	444
	5000	166.7	2	1.27E+06	1.72E+06	483	432

Tab.2: Identified stiffness and damping coefficients of bearing 1

Identified stiffness and damping elements of test bearing 2 are summarized in Table 3. Excitation frequency of 30 Hz was used for all speeds, because with higher frequencies the signals of bearing response were somewhat distorted and condition of harmonic excitation was not therefore fulfilled. It can be seen, that in accordance with quasi-static values of stiffness also elements K_{xx} and K_{yy} of bearing 2 differ with roughly the same ratio.

Inlet pressure (MPa)	speed n (rpm)	excitation frequency f (Hz)	ratio r	K_{xx} (N.m ⁻¹)	K_{yy} (N.m ⁻¹)	B_{xx} (N.s.m ⁻¹)	B_{yy} (N.s.m ⁻¹)
0.2	0	30	—	2.45E+06	1.33E+06	618	997
	1000	30	1.8	2.35E+06	1.25E+06	759	1030
	2000	30	0.9	2.31E+06	1.15E+06	721	1110
	3000	30	0.6	2.32E+06	1.16E+06	774	1170
	4000	30	0.45	2.24E+06	1.14E+06	699	1060
	5000	20	0.24	2.17E+06	1.17E+06	668	1070
0.4	6000	30	0.3	2.16E+06	1.15E+06	498	1210
	0	30	—	5.25E+06	3.77E+06	789	1090
	1000	30	1.8	5.19E+06	4.09E+06	901	855
	2000	30	0.9	4.83E+06	3.22E+06	1810	1450
	3000	30	0.6	4.70E+06	3.31E+06	466	955
	4000	30	0.45	4.54E+06	3.11E+06	1685	1179
5000	30	0.36	4.66E+06	3.33E+06	582	1080	
	6000	30	0.3	4.65E+06	3.40E+06	349	995

Tab.3: Identified stiffness and damping coefficients of bearing 2

Table 4 presents eigenfrequencies and eigendampings calculated from identified complete stiffness and damping matrices of bearing 2. Contrary to principal stiffness and damping elements, eigenfrequencies (imaginary parts of complex eigenvalues) and eigendampings (absolute values of real part of complex eigenvalues) were calculated from identified non-diagonal elements of corresponding matrices. Variability of non-diagonal elements of stiffness and namely damping matrices (together with prevailing diagonal matrix elements) implicates the alternations in eigenfrequencies and eigendampings, mostly in the case of higher inlet pressure of 0.4 MPa (see Table 4). All calculated eigenvalues correspond to stable mathema-

Inlet pressure (MPa)	speed n (rpm)	excitation frequency f (Hz)	ratio r	1 st eigen-frequency (Hz)	1 st eigen-damping (Hz)	2 nd eigen-frequency (Hz)	2 nd eigen-damping (Hz)
0.2	0	30	-	153	65	225	42
	1000	30	1.8	147	69	217	49
	2000	30	0.9	137	80	212	40
	3000	30	0.6	136	78	215	50
	4000	30	0.45	141	72	210	45
	5000	20	0.24	143	73	207	43
0.4	6000	30	0.3	135	85	209	28
	0	30	-	272	73	329	52
	1000	30	1.8	289	56	325	60
	2000	30	0.9	264	88	271	128
	3000	30	0.6	256	65	315	30
	4000	30	0.45	209	78	288	111
	5000	30	0.36	256	73	310	37
	6000	30	0.3	258	68	312	21

Tab.4: Eigenfrequencies and eigendampings calculated from identified stiffness and damping matrices of bearing 2

tical model (with negative real parts) and relative damping values are in intervals $\langle 0.4, 0.6 \rangle$, $\langle 0.1, 0.2 \rangle$ for inlet pressure of 0.2 MPa and $\langle 0.2, 0.3 \rangle$, $\langle 0.1, 0.5 \rangle$ for inlet pressure of 0.4 MPa respectively.

6. Comparison of experimental and calculated results

Identified ‘quasi-static’ and dynamic stiffness coefficients enabled to revise computer program for aerostatic journal bearings. Detailed description of theoretical solution and computer program can be found in [6]. Results of revised program calculation were then compared with experimental values. Apart from experimental data from RK test stand, also load-eccentricity characteristics from work [4] were used for comparison, because it included rotating speeds up to more 50000 rpm, showing already strong influence of journal rotation speed on load capacity of the bearing. As can be seen from Fig. 8, qualitative as well as quantitative agreement between revised program calculation and experimental results is quite good for both values of inlet pressure of 0.2 MPa (left) and 0.4 MPa (right). Similarly good agreement was obtained also for smaller value of bearing clearance of 0.018 mm, where maximum achieved speed was 53500 rpm.

Comparison of measured stiffness coefficients of bearing 1 with values calculated after computer program revision is presented in Table 5. It is evident, that agreement of calculated results with experimental ones is reasonably good. Calculated damping coefficient agreed quite well with experimental data already before program revision for excitation ratio around 1. Contrary to calculation the experimental results did not show strong dependence of damping on excitation ratio. This fact is also respected in revised program.

7. Spectral and modal properties of mathematical model

As an example of identified mathematical model let us present experimentally determined matrices of stiffness and damping, corresponding to zero speed and inlet pressure of 0.2 MPa for bearing 1 (\mathbf{K}_1 , \mathbf{B}_1) and bearing 2 (\mathbf{K}_2 , \mathbf{B}_2). Spectral (complex eigenvalues in

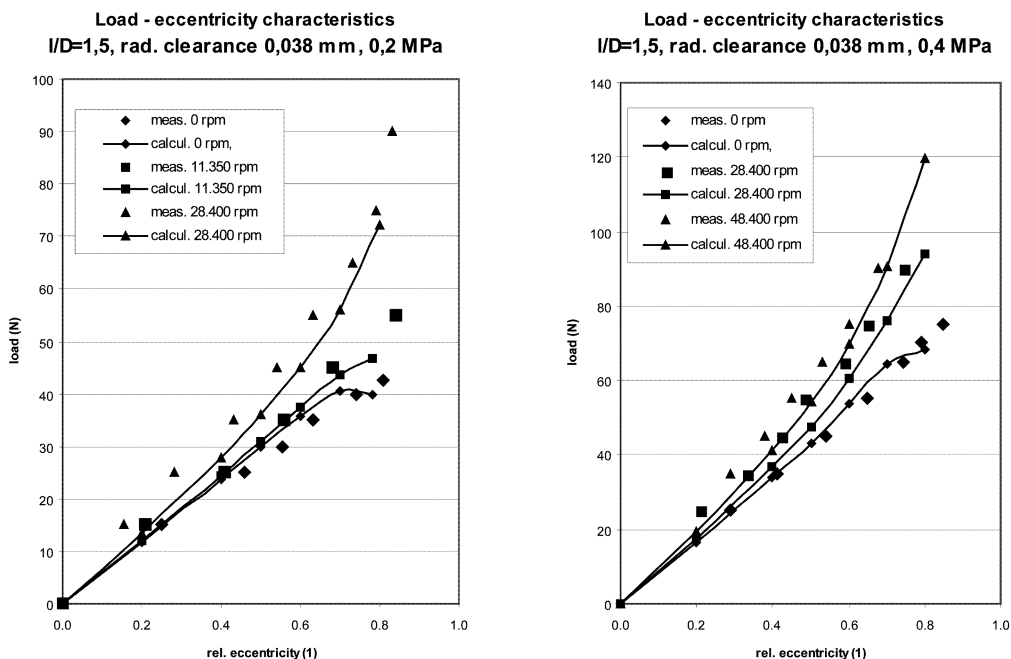


Fig.8: Comparison of calculated and measured load capacity vers. relative eccentricity

Inlet pressure (MPa)	speed n (rpm)	excitation frequency f (Hz)	ratio r	measured		calculated	
				K_{xx} (N.m ⁻¹)	K_{yy} (N.m ⁻¹)	K_{xx} (N.m ⁻¹)	K_{yy} (N.m ⁻¹)
0.2	0	5	—	9.52E+05	9.65E+05	1.02E+06	1.00E+06
	1000	16.7	1	9.88E+05	9.79E+05	1.02E+06	1.01E+06
	2000	66.7	2	9.30E+05	9.79E+05	1.02E+06	1.01E+06
	3000	25	0.5	1.00E+06	9.66E+05	1.02E+06	1.01E+06
	4000	33.3	0.5	9.84E+05	9.77E+05	1.02E+06	1.02E+06
	5000	41.7	0.5	9.51E+05	9.71E+05	1.02E+06	1.01E+06
0.4	0	5	—	1.42E+06	1.41E+06	1.52E+06	1.51E+06
	1000	8.3	0.5	1.43E+06	1.45E+06	1.52E+06	1.51E+06
	2000	16.7	0.5	1.43E+06	1.44E+06	1.52E+06	1.51E+06
	3000	25	0.5	1.42E+06	1.42E+06	1.53E+06	1.51E+06
	4000	33.3	0.5	1.44E+06	1.45E+06	1.53E+06	1.51E+06
	5000	166.7	2	1.27E+06	1.72E+06	1.53E+06	1.51E+06

Tab.5: Comparison of calculated and measured principal stiffness coefficients

diagonals of spectral matrices \mathbf{S}_1 , \mathbf{S}_2) and modal (right modal matrices \mathbf{V}_1 , \mathbf{V}_2 and left modal matrices \mathbf{W}_1 , \mathbf{W}_2 with normed vectors – columns – conformed with the condition, that in absolute value bigger coordinates of right- and left-eigenvectors are identical) matrices were calculated for both models. Influence of non-diagonal elements of stiffness and damping matrices \mathbf{K}_1 , \mathbf{B}_1 of mathematical model of the bearing 1 will be further analyzed by means of numerical simulation.

Both identified mathematical models have non-symmetric stiffness and damping matrices with $K_{xy} \neq K_{yx}$ and $B_{xy} \neq B_{yx}$, which, as will be shown later, with regard to substantially predominating diagonal elements (main stiffness elements) do not have significant influence

on their dynamic properties, and damping matrices, of which do not differ too much from so called commutative matrix (i.e. with eigenvectors nearing corresponding undamped system).

Coefficient matrices for bearing 1 are

$$\mathbf{M} = \begin{bmatrix} 1.2 & 0 \\ 0 & 1.2 \end{bmatrix}, \quad \mathbf{K}_1 = \begin{bmatrix} 952000 & 12700 \\ 10900 & 965000 \end{bmatrix}, \quad \mathbf{B}_1 = \begin{bmatrix} 525 & -10.1 \\ 16 & 698 \end{bmatrix},$$

complex diagonal spectral matrix (in Hz)

$$\mathbf{S}_1 = \begin{bmatrix} -46.2 + 135.1 i & 0 \\ 0 & -34.9 + 137.4 i \end{bmatrix}$$

shows stable dynamic system with higher relative damping and with eigenfrequencies of vibration in vertical and horizontal directions close one to the other, which are substantially higher than frequency of forced vibrations from prospective unbalances at shaft speeds up to 6000 rpm.

Modal matrices are complex, but after division by the number $(1 - i)$ we get eigenvectors close to real ones and it is evident, that damping matrix is almost commutative and further, that 'asymmetry' of the model characterized by difference of right- and left-eigenvectors is small:

$$\mathbf{V}_1 = \begin{bmatrix} -0.0027 - 0.0001 i & 0.0156 - 0.0156 i \\ 0.0158 - 0.0157 i & -0.0003 + 0.0023 i \end{bmatrix},$$

$$\mathbf{W}_1 = \begin{bmatrix} 0.0002 - 0.0022 i & 0.0156 - 0.0156 i \\ 0.0158 - 0.0157 i & 0.0025 - 0.0002 i \end{bmatrix}.$$

Coefficient matrices for bearing 2 are

$$\mathbf{M} = \begin{bmatrix} 1.2 & 0 \\ 0 & 1.2 \end{bmatrix}, \quad \mathbf{K}_2 = \begin{bmatrix} 2162649 & 65224 \\ 4935 & 1213610 \end{bmatrix}, \quad \mathbf{B}_2 = \begin{bmatrix} 822 & -71 \\ -99 & 1173 \end{bmatrix},$$

with similar properties as before, but now with substantially higher stiffness in vertical direction of vibration, which manifests also by corresponding higher eigenfrequency - see imaginary parts of spectral matrix (in Hz):

$$\mathbf{S}_2 = \begin{bmatrix} -78.5 + 139.7 i & 0 \\ 0 & -53.8 + 206.5 i \end{bmatrix}.$$

Conclusions similar to those for bearing 1 are valid also for right and left modal matrices of bearing 2:

$$\mathbf{V}_2 = \begin{bmatrix} -0.0011 + 0.0019 i & 0.0127 - 0.0126 i \\ 0.0154 - 0.0153 i & -0.0002 + 0.0021 i \end{bmatrix},$$

$$\mathbf{W}_2 = \begin{bmatrix} -0.0001 + 0.0019 i & 0.0127 - 0.0126 i \\ 0.0154 - 0.0153 i & 0.0008 - 0.0018 i \end{bmatrix}.$$

As identified, namely non-diagonal elements of stiffness and damping matrices, showed great differences in identification, their influence on spectral properties was examined by the way of numeric simulation and with the help of inverse formulae derived for this model with coefficient matrices of the 2nd order in analytic form - [5]. We proceeded by inverse method, when for selected, relatively small interval of variation of eigendamping $|\operatorname{Re}(s_1)|$

$\text{Re}(s_1) \in \langle -55.7, -39.8 \rangle$	$\text{Im}(s_1) \in \langle 127.3, 143.2 \rangle$
$K_{xx} \in \langle 951920, 952070 \rangle$	$K_{xx} \in \langle 950620, 953330 \rangle$
$K_{xy} \in \langle 7324, 20512 \rangle$	$K_{xy} \in \langle 1510, 2300 \rangle$
$K_{yx} \in \langle 3465, 22526 \rangle$	$K_{yx} \in \langle 4371, 18216 \rangle$
$K_{yy} \in \langle 938900, 1011500 \rangle$	$K_{yy} \in \langle 867600, 1074200 \rangle$
$B_{xx} \in \langle 523.4, 526.1 \rangle$	$B_{xx} \in \langle 524.7, 525.3 \rangle$
$B_{xy} \in \langle -20.34, -2.75 \rangle$	$B_{xy} \in \langle -20.9, 0.8 \rangle$
$B_{yx} \in \langle 8.28, 27.01 \rangle$	$B_{yx} \in \langle 7.96, 23.16 \rangle$
$B_{yy} \in \langle 600.8, 843.5 \rangle$	$B_{yy} \in \langle 697.7, 698.2 \rangle$

Tab.6: Prescribed variation of $\text{Re}(s_1)$ and $\text{Im}(s_1)$ and corresponding changes of elements of coefficient matrices \mathbf{K}_1 , \mathbf{K}_2

and of eigenfrequency $\text{Im}(s_1)$ of bearing model 1, corresponding intervals of values of all elements of the matrices \mathbf{K}_1 , \mathbf{B}_1 were calculated – Table 6.

It follows from Tab. 6, that relatively small changes of diagonal (main) elements of coefficient matrices and much greater changes of non-diagonal elements correspond to selected intervals of spectral changes. As spectral values actually define dynamic properties of the model and its response, this means, that greater variability of non-diagonal elements in identification evaluation of measured, by experimental errors burdened responses, is a consequence of their smaller influence on forced vibrations.

8. Conclusions

Project of aerostatic journal bearing dynamic properties identification was carried out, using superstructure built on Rotor Kit Bently Nevada. Although maximum achievable journal speed was limited to about 6 000 rpm, it was possible to attain sufficient quantity of measured data. That enabled to revise computer program, so that reasonable agreement between calculation and experiment was achieved. As no experimental data concerning stiffness and damping of aerostatic journal bearings were available before, important step in verification of aerostatic journal bearing computational methods was made.

Acknowledgement

This work was supported by the Czech Science Foundation under project No. 101/06/1787 ‘Dynamic properties of gas bearings and their interaction with rotor’.

References

- [1] Kozánek J., Šimek J., Steinbauer P., Bílkovský A.: Identification of aerostatic journal bearing stiffness and damping, Colloquium Dynamics of Machines 2009, p. 37
- [2] Šimek J., Kozánek J., Steinbauer P., Neusser Z.: Determination of aerostatic journal bearing properties, Colloquium Dynamics of Machines 2008, p. 169
- [3] Šimek J., Kozánek J., Steinbauer P.: Dynamic properties of aerostatic journal bearings, Colloquium Dynamics of Machines 2007, p. 177
- [4] Šimek J.: Hybrid journal gas bearings with stationary flow in the film, Research report No. SVÚSS 77-06006, 1977 (in Czech)
- [5] Kozánek J.: Analytic formulae for the construction of diagonalisable dynamical systems, Proc. of XV-th National seminar Interaction and Feedbacks 2008, p. 47 (in Czech)
- [6] Šimek J., Kozánek J.: Identification of aerostatic journal bearings dynamic properties. Part 2: Comparison of measured static and dynamic characteristics with calculation. Description of

methodology of solution and computer program revision. Technical report Techlab No. 08-411, 2008 (in Czech)

- [7] Kozánek J.: Remark on least squares problem in identification solutions, Proc. Colloquium Dynamics of Machines 95, IT AV CR, Prague ÚT, pp. 55–60, 1995 (in Czech)
- [8] Daněk O., Balda M., Turek F., Zeman V., Kozánek J.: Dynamics of non-conservative systems, Czechoslovak Society for Mechanics CAS, Brno, 1986 (in Czech)

Received in editor's office: March 18, 2009

Approved for publishing: June 23, 2009

Note: This paper is an extended version of the contribution presented at the national colloquium with international participation *Dynamics of Machines 2009* in Prague.